



Article

Quantifying CO₂ Emissions and Carbon Sequestration from Digestate-Amended Soil Using Natural ¹³C Abundance as a Tracer

Gregory Reuland ^{1,2,*} , Steven Sleutel ³, Haichao Li ⁴, Harmen Dekker ², Ivona Sigurnjak ¹ and Erik Meers ¹ 

¹ Department of Green Chemistry and Technology, Faculty of Bioscience Engineering, Ghent University, Coupure Links 653, 9000 Ghent, Belgium

² European Biogas Association, Rue d'Arlon 65, 1050 Brussels, Belgium

³ Department of Environment, Faculty of Bioscience Engineering, Ghent University, Coupure Links 653, 9000 Gent, Belgium

⁴ Department of Soil and Environment, Swedish University of Agricultural Sciences, Lennart Hjelms väg 9, 750 07 Uppsala, Sweden

* Correspondence: gregory.reuland@ugent.be or gregory.reuland@gmail.com

Abstract: The untapped potential for carbon sequestration in agricultural soils represents one of the most cost-effective tools for climate change mitigation. Increasing soil organic matter also brings other agronomic benefits such as improved soil structure, enhanced water-and-nutrient-retention capacity, and biological activity. Broadly, soil organic carbon storage is achieved by increasing carbon inputs (plant residues and organic amendments) and reducing carbon outputs (soil loss mechanisms, decomposition). With a focus on carbon inputs—more specifically, organic amendments—as leverage to increase soil organic carbon, we compared the respiration rates and carbon storage of incubated soil cores amended with maize straw, manure, two digestates and the solid fraction of digestate. Using the variation in the natural ¹³C abundance found in C₄ and C₃ plants as a tracer, we were able to partition the CO₂ emissions between the exogenous organic matter materials elaborated from maize (C₄) and native soil organic carbon (C₃). The addition of digestate resulted in an additional 65 to 77% of remaining organic carbon after 92 days. The digestate-derived CO₂ was fitted to a second-order kinetic carbon model that accounts for the substrate C that is assimilated into the microbial biomass. The model predicted a carbon sequestration potential of 56 to 73% of the total applied organic carbon after one to two years. For the solid fraction, the results were higher, with 89% of the applied organic carbon after 92 days and a sequestration potential of 86%. The soil priming ranged from −19% to +136% in relation to the unamended control soil, highlighting a surprisingly wide spectrum of results that warrants the need for further research on soil–digestate interactions.

Keywords: stable carbon isotope; priming effect; soil organic carbon; nitrates directive



Citation: Reuland, G.; Sleutel, S.; Li, H.; Dekker, H.; Sigurnjak, I.; Meers, E. Quantifying CO₂ Emissions and Carbon Sequestration from Digestate-Amended Soil Using Natural ¹³C Abundance as a Tracer. *Agronomy* **2023**, *13*, 2501. <https://doi.org/10.3390/agronomy13102501>

Academic Editor: Wenjie Wan

Received: 11 September 2023

Revised: 26 September 2023

Accepted: 27 September 2023

Published: 28 September 2023



Copyright: © 2023 by the authors. Licensee MDPI, Basel, Switzerland. This article is an open access article distributed under the terms and conditions of the Creative Commons Attribution (CC BY) license (<https://creativecommons.org/licenses/by/4.0/>).

1. Introduction

Digestate is the leftover organo-mineral material following the anaerobic digestion (AD) of organic feedstocks (manure, municipal waste, crop residues) to produce biogas. In reason of its high content of nutrients in mineral form, primarily nitrogen (N), phosphorus (P) and potassium (K) [1,2], digestate can be used directly as a fertiliser, all the while increasing the share of recycled nutrients recovered from organic waste streams in the context of a circular economy model [3]. In the frame of the European Union's (EU's) objective to reach climate neutrality by 2050, embodied in the Green Deal, the biogas sector has been picking up steam in recent years as a rapidly deployable solution for renewable energy. The recent *REPowerEU* Plan to rapidly phase out European dependence on fossil fuels further accelerates the rollout of renewable energy. These measures, aimed at ramping up biogas production, imply that larger volumes of digestate need to find

a suitable outlet [4]. The further biorefining of digestate to isolate nutrients offers one such solution [5,6]; however, the most common use for digestate remains direct land spreading [7].

While many studies have focused on the N-fertilising properties of digestate as an alternative to synthetic fertilisers [8–10], an interesting aspect worth considering for agricultural soils is that digestate also carries carbon (C). The 4 per 1000 initiative, instigated by the French government at the COP21 Paris Climate Summit in 2015, underpins the importance of increased soil C storage as a climate mitigation strategy to reduce atmospheric CO₂ and improve soil health, water retention, resilience, and, in turn, food security [11]. As a possible input of C, the physicochemical properties of digestate can vary considerably in reason of the composition and different ratios of the input feedstocks [12] and of the specific parameters of the AD process (retention time, temperature), both of which have been shown to affect digestate C and N mineralisation [13,14]. Recalcitrant forms of C concentrate in digestate as a consequence of the labile C contained in the feedstocks being more favourably converted into biogas by the microbial consortia during the AD process [14–16]. Consequently, digestate may hold promise as an input of C for increasing soil organic carbon (SOC) stocks, as also underlined in several studies [17–21]. Nevertheless, the addition of digestate has also been reported to have no discernible effects [22]. Either way, there is little information on the interactions between digestate and native soil organic matter (SOM) via so-called priming effects (PEs), a key component of global C cycling [23], which can be defined as a change in SOM decomposition in response to fresh organic matter (OM) input to soil [24]. The overarching objective was to benchmark the mineralisation rates of digestate next to common exogenous organic matter (EOM) materials and shed new light on the potentially sequestered C and agronomic implications of using digestate as C-input for soils. Limited insight into digestate behaviour in soil results particularly from the difficulty in resolving SOM from digestate C mineralisation, as the production of digestate with a contrasting stable C-isotopic composition is unstraightforward and, moreover, contains inorganic carbon, which contributes to the overall soil CO₂ efflux. To bridge this knowledge gap, the variation in the natural ¹³C abundance found in C₄ and C₃ plants was used as a tracer to effectively allocate soil CO₂ emissions between EOM materials, including digestate, elaborated from a C₄ plant (*Zea mays* L.), on one hand, and soil that bore C₃ plants, on the other. Because differences in natural abundance are relatively limited, we accounted for the dynamics in isotopic fractionation during soil C mineralisation and CO₂ efflux in a soil incubation experiment.

2. Materials and Methods

2.1. Materials Collection and Experimental Design

Two subsoils, chosen for their low SOC contents of 6 and 1 g kg^{−1} (Table 1), were collected in the East Flanders province of Belgium. For ease of reference, the soils (S) were named after their SOC contents, namely, S_{0.6} and S_{0.1} (Table 1). The former was sampled from arable land in Kruisem (50°55′ 43.3″ N, 3°32′55.4″ E) at a depth of 0.2–0.4 m, and the latter was sampled at a depth of 0.5–1.0 m from a permanent pasture located in Merelbeke (50°59′43.9″ N, 3°45′38.9″ E). The soils are characterised, respectively, as loamy sand and sand [25,26]. The soils were air-dried, sieved through a 2 mm mesh and stored at room temperature. Any gravel and plant debris were carefully removed by hand. For the sake of clarity, the mention of control soil hereafter (labelled CL, described further below) refers exclusively to the use of S_{0.6} (Table 1). The S_{0.6} soil was used for the main experiment, which lasted 92 days. The S_{0.1} was used in a parallel, shorter incubation experiment of 21 days, to assess isotopic fractionation during EOM mineralisation as detailed hereafter (Section 2.4).

Table 1. Soil main physicochemical characteristics.

Parameter	Unit	Loamy Sand (S _{0,6})	Sand (S _{0,1})
pH _{KCl}	/	6.5 ± 0.0	4.1 ± 0.0
pH _{H2O}	/	6.8 ± 0.1	5.5 ± 0.0
EC	mS cm ^{−1}	0.03 ± 0.00	0.06 ± 0.00
TN	g kg ^{−1}	0.63 ± 0.06	0.12 ± 0.02
TC	g kg ^{−1}	5.9 ± 0.0	1.0 ± 0.1
SOC	g kg ^{−1}	5.8 ± 0.0	1.0 ± 0.0
Sand	%	84	92
Silt	%	13	6
Clay	%	3	2
δ ¹³ C	‰	−25.2	−26.4
C/N	/	9.4	8.5

EC = electrical conductivity; TN = total nitrogen; TC = total carbon; SOC = soil organic carbon; δ¹³C = ¹³C isotope analysis of dry substrate. For additional soil physicochemical data, see Table S1.

The EOM-amending materials used in this experiment consisted of maize straw (MZ), cattle manure (MN), two digestates (DG1 and DG2) and the solid fraction of digestate (SF). The maize straw (*Zea mays* L.), composed of dry maize shoots and leaves, was roughly chopped into 1 to 2 cm long pieces. The MN was collected from a cattle farm in Hondeghem, Hauts-de-France, France, where cows received 56% fresh maize in their daily feed intake. A full-scale biogas plant in Neuried, Baden-Württemberg, Germany, provided DG1 and the SF, where the AD temperature was kept at 48 °C with a total retention time of 29 days. This is a two-stage AD process featuring a hydrolysis reactor (1200 m³) and a methanogenesis reactor (550 m³). The SF corresponded to the dewatered fraction of DG1, obtained by pouring DG1 onto the greenhouse floor to reach a thickness of 15–20 cm, after which it was heated to 50–80 °C (depending on weather conditions) for four weeks with the thermal energy generated from the combined heat and power unit. The DG2 was obtained from a full-scale biogas plant located in Titz, Düren, Germany (ADRW NaturPower GmbH & Co. KG). It came from a single-stage AD maintained at 52 °C in a 2500 m³ digester tank with a hydraulic retention time of 72 days. All digestates (DG1, DG2 and SF) contained >95% maize as feedstock. All samples were collected in polyethylene sampling bottles and stored at 4 °C until further use.

The five EOM treatments—MZ, MN, SF, DG1, DG2—were each prepared in triplicate, and, serving as control (CL), unamended soil without EOM was prepared in quintuplicate, totalling 20 tubes. As previously stated, the soil that served as CL was S_{0,6} (Table 1). The EOM materials were thoroughly mixed with 254.2 g of dry soil at an equivalent rate of 2.5 t total organic carbon (TOC) ha^{−1}, which corresponded to 1.19 g_{MZ}, 7.65 g_{MN}, 1.19 g_{SF}, 10.82 g_{DG1} and 16.26 g_{DG2} of added fresh matter, respectively. As a first step, the soil was preincubated in a dark room at a constant temperature of 20 °C for 10 days at 35% water-filled pore space (WFPS). After that, the EOM materials were mixed into the soil and gently packed to reach a height of 5 cm and a bulk density of 1.4 g cm^{−3} in polyvinyl chloride (PVC) tubes measuring 6.8 cm in diameter and 7 cm in height. For the semi-solid EOMs (MN, DG1, DG2), a magnetic stirrer was used to homogenise the materials prior to their addition to the soil. The water content of each EOM material was considered to reach 50% WFPS in the final soil cores. Each mesocosm was placed inside a leakproof glass jar (1 L). In each jar, a vial (120 cm³) containing 30 mL of 1 M sodium hydroxide (NaOH) was included. Although the glass jars were sealed shut once inside the incubation cabinet, the NaOH traps were inserted as an extra precaution to avoid any CO₂ cross-contamination between treatments. The jars containing the mesocosms were then randomly positioned inside an incubation cabinet at a constant temperature of 20 °C during the 92 days of the experiment. At regular intervals, the NaOH solutions were changed, and the glass jars were individually opened and placed in front of a fan at full speed for about 20' under a fume hood to ensure complete air renewal. Each soil core was taken out and placed back

inside the incubation cabinet one at a time to ensure that no open soil core was ever in close contact with another. The gravimetric water content was registered at 50% WFPS and readjusted with demineralised water every 2 to 5 days.

At the end of the incubation (day 92), a series of destructive analyses was performed on each of the 20 incubated soil cores, i.e., the quintuplicate control soils and the triplicates of the five EOM treatments. In this way, the microbial biomass carbon (MBC), the gravimetric water content, pH_{KCl} and residual mineral N were all determined in homogenised samples taken from each of the fresh soil cores on day 92 (Section 2.3).

2.2. Measurement of CO_2 Fluxes

For the CO_2 measurements, an airtight static flux chamber was fastened to the rim of the PVC tube containing the soil core. The flux chamber was fitted with two bulkhead connectors and PTFE tubing connected in a closed loop to an external vacuum pump, itself connected to a calibrated cavity ring-down spectroscopy analyser (G2201-i CRDS isotopic CO_2/CH_4 analyser, Picarro, Santa Clara, CA, USA). This setup allowed us to measure the build-up of CO_2 in the headspace (370 cm^3) and the variations in $^{12}\text{CO}_2$ and $^{13}\text{CO}_2$ efflux rates from the mesocosms over time. The duration of measurement was never inferior to 8' per mesocosm and was adapted for each treatment according to the velocity of the observed cumulative CO_2 build-up in the headspace. In all instances, excessive CO_2 build-up in the headspace leading to non-linear efflux was avoided. Measurements were taken on twelve separate occasions over the course of the 92-day experiment: on days 1, 3, 7, 9, 13, 15, 21, 28, 37, 48, 64 and 92. After a measurement was taken on a soil core, and before measuring the next, enough time was allowed for the CO_2 readings to return to ambient levels ($\pm 416 \text{ ppm CO}_2$). The measurements of soil cores were systematically carried out in a completely randomised pattern.

A linear model was fitted to the measured CO_2 build-up as a function of time to determine the CO_2 effluxes (ppm s^{-1}). These volumes of CO_2 were then converted to mass ($\text{mg CO}_2\text{-C h}^{-1}$) using the ideal gas law. The Keeling plot method was applied [27], which considers the isotopic $\delta^{13}\text{C}$ signature of emitted CO_2 as the y-intercept of the linear regression function of the measured $\delta^{13}\text{C}$ values as a function of the inverse of the CO_2 headspace concentration.

2.3. Physicochemical Characterisations

Total carbon (TC), TOC and total nitrogen (TN) were measured using a PRIMACS100 Analyser series (Skalar Analytical BV, Breda, The Netherlands). The pH_{KCl} was determined using an Orion Star A211 pH electrode (Thermo Fisher Scientific, Waltham, MA, USA) placed in a 1/5 ratio (w/v) of fresh sample to 1 M potassium chloride (KCl). For $\text{pH}_{\text{H}_2\text{O}}$, the sample was prepared in the same ratio with demineralised water instead. The suspension was mixed for 60' on an orbital shaker and left to settle overnight before taking the reading. Electrical conductivity (EC) was measured with an Orion Star A212 conductivity meter in a 1/5 ratio (w/v) of fresh sample to demineralised water. The suspension was placed on an orbital shaker for 60' and filtered (Whatman No. 43, Maidstone, UK) prior to the reading. Dry matter (DM) was determined using the gravimetric difference between the fresh and oven-dried samples at 105°C . The residual ammonium N ($\text{NH}_4^+ - \text{N}$) and nitrate N ($\text{NO}_3^- - \text{N}$) in the incubated soil cores were measured from filtrates, prepared in a 1/5 ratio (w/v) of fresh sample to 1 M KCl, on a Skalar SA 1050 flow injection analyser. For measuring $\text{NH}_4^+ - \text{N}$ content in the EOM materials, the samples were prepared in a 1/5 ratio (w/v) of fresh sample to demineralised water, to which magnesium oxide (MgO) was added. The samples were then distilled in a Vapodest 20 distillation unit (Gerhardt, Gemini BV, Apeldoorn, The Netherlands). The distilled NH_4^+ was trapped in a 2% boric acid solution (H_3BO_3) titrated with 0.05 M hydrochloric acid (HCl) on an automatic 718 Stat Titrino titrator (Metrohm, Herisau, Switzerland). The $\delta^{13}\text{C}$ isotope signature of the materials was measured with EA-IRMS using an ANCA-SL (Automated Nitrogen Carbon Analyser-Solids and Liquids) interfaced with a SerCon 20–22 IRMS (SysCon electronics, Cheshire, UK).

Soil texture was determined using the pipette sedimentation method [28]. The MBC was determined using the chloroform fumigation-extraction method on 30 g of soil [29]. The potassium sulphate (K_2SO_4) 0.1 M filtrates were measured using a Formacs^{HT-I} TOC/TN analyser (Skalar Analytical BV, Breda, The Netherlands). The difference in extractable C between the fumigated and non-fumigated samples was considered as the MBC. A correction coefficient of 0.45 was factored into account for the fraction of the fumigated C-biomass that was mineralised to CO_2 -C [30]. Total P, sulphur (S), K, sodium (Na), magnesium (Mg), calcium (Ca), aluminium (Al), iron (Fe), cadmium (Cd), copper (Cu) and zinc (Zn) were determined in 0.1 g of dry, ground sample (<250 μm) with nitric acid digestion (HNO_3 65%) using a Varian Vista MPX Simultaneous ICP-OES (Varian Inc., Palo Alto, CA, USA). Dissolved organic carbon (DOC) was determined following the Macherey–Nagel protocol reference 985,093 [31] using a filter pore size of 0.45 μm . Acid detergent fibre (ADF) and acid detergent lignin (ADL) were analysed to determine the contents of lignin and cellulose, respectively, following the Van Soest method [32]. The DOC and Van Soest characterisations were performed by a certified laboratory (Innolab, Oostkamp, Belgium). Additional physicochemical properties of the exogenous organic matter materials are presented in Table S2.

2.4. Calculations

The different fractions of CO_2 -C emitted from a particular mesocosm were calculated based on the following mixed model equation [33], which takes into consideration $\delta^{13}C$ of CO_2 emissions from the EOM treatment and the control soil (CL):

$$CO_2-C_{EOM} = CO_2-C \times \frac{\delta^{13}C-CO_2 (EOM_{0.6}) - \delta^{13}C-CO_2 (CL)}{\delta^{13}C-CO_2 (EOM_{0.1}) - \delta^{13}C-CO_2 (CL)} \quad (1)$$

where CO_2-C_{EOM} is the amount of CO_2 -C derived from the added EOM ($mg\ CO_2-C\ kg^{-1}\ soil\ 24\ h^{-1}$); CO_2-C represents the total amount of evolved CO_2 -C from the mesocosm ($mg\ CO_2-C\ kg^{-1}\ soil\ 24\ h^{-1}$); $\delta^{13}C-CO_2(EOM_{0.6})$ is the isotopic $\delta^{13}C$ signature of CO_2 emitted from the EOM-amended mesocosm determined with Keeling plots using the $S_{0.6}$ soil (Table 1); $\delta^{13}C-CO_2(CL)$ is the estimated isotopic $\delta^{13}C$ signature of CO_2 emitted from the CL soil (corresponding to unamended $S_{0.6}$, Table 1) resulting from SOC mineralisation only; and $\delta^{13}C-CO_2(EOM_{0.1})$ is the estimated isotopic $\delta^{13}C$ signature of emitted CO_2 assumed to derive from EOM only, i.e., with EOM added in a large amount in the low SOC $S_{0.1}$ soil (Table 1). Indeed, to better account for isotopic fractionation, a parallel experiment was set up with the exact same parameters, conditions and treatments (Section 2.1), but with $S_{0.1}$ soil instead of $S_{0.6}$ (containing 0.1% instead of 0.6% SOC, Table 1). The measurements of CO_2 effluxes from the EOM treatments using $S_{0.1}$ soil were taken on the same days (1, 3, 7, 9, 13, 15, 21) as the main experiment. This experiment lasted 21 days, which corresponded to the moment when the cumulative mineralised C from the 92-day experiment with $S_{0.6}$ exhibited a linear trend (Figure S1). Hence, from days 1 to 21, the value of the endmember $\delta^{13}C-CO_2(EOM_{0.1})$ (Equation (1)) was taken from the estimated isotopic $\delta^{13}C$ signature of CO_2 emitted from the EOM treatments using $S_{0.1}$ soil on each of those days (days 1, 3, 7, 9, 13, 15, 21). From day 21 onwards, it was assumed that the $\delta^{13}C$ value measured on day 21 was representative of all biological activity after that point and that only one pool of C was contributing to CO_2 emissions, as indicated by the linear trend in cumulative C mineralisation showcased over the 92-day incubation. Consequently, from days 21 to 92, the endmember $\delta^{13}C-CO_2(EOM_{0.1})$ was locked on the isotopic $\delta^{13}C$ signature of CO_2 of day 21.

Subsequently, the fraction of CO_2 -C emitted from the EOM-amended soil (CO_2-C_{soil} , Equation (2)) was calculated as the difference between CO_2-C_{EOM} and the total amount of evolved CO_2 -C from the mesocosm (as defined in Equation (1)), expressed in $mg\ CO_2-C\ kg^{-1}\ soil\ 24\ h^{-1}$:

$$CO_2-C_{soil} = CO_2-C - CO_2-C_{EOM} \quad (2)$$

From that point, the intensity and direction of the PE were expressed as a percentage of cumulative CO_2 emitted by the treatment soil (CO_2-C_{soil}) relative to the amount of cumulative CO_2 emitted by the unamended control soil (CO_2-C_{CL}) [34] on day 92:

$$PE (\%) = \frac{CO_2-C_{soil} - CO_2-C_{CL}}{CO_2-C_{CL}} \times 100 \quad (3)$$

The EOM-derived CO_2-C was expressed as a percentage of added TOC from the EOM materials. A second-order kinetic model [35] was fitted to the results of the cumulative C mineralised from the EOM materials to extrapolate the amount of unmineralised TOC after 1 to 2 years as a proxy for the potentially sequestered C ($TOC_{seq-EOM}$ hereafter):

$$C(t) = C_A - \frac{C_A}{1 + k_2 a (1 - a) C_A t} \quad (4)$$

where $C(t)$ is the cumulative amount of C mineralised at time t ; C_A is the amount of mineralised C; k_2 is the second-order mineralisation rate; a is the amount of mineralised substrate C that becomes part of the microbial biomass itself and further influences the mineralisation process. Variables k_2 and a are expressed as a single variable $k_2 a (1 - a)$ (see Table S3 for parameters from the second-order kinetic model).

2.5. Statistical Analyses

All experiments and physicochemical characterisations were performed in triplicate, with the exception of the untreated control soil (CL), which was prepared in quintuplicate. The data are presented as the mean \pm standard deviation. One-way ANOVA and Tukey's post hoc test at $p < 0.05$ were used to highlight differences in C and N mineralisation rates, MBC and pH between the different EOM treatments. The Shapiro–Wilk test was used to check the normal distribution of the continuous variables. The equality of variances between EOM treatments was checked using Levene's test. In the cases where assumptions of a normal distribution and equal variance were violated, the data were analysed using the nonparametric Kruskal–Wallis one-way analysis of variance, followed by Dunn's post hoc test with Bonferroni correction. Correlation coefficients between treatment results and physicochemical properties of EOM materials were determined using Pearson's correlation. A one-sample T -test ($p < 0.05$) was carried out to determine if the PE (Equation (3)) of the treatments was significantly different from that of the control soil (test value of 0). All statistical analyses were carried out on SPSS 27.0 software 64-bit edition (IBM Corp, Armonk, NY, USA) for Windows.

3. Results

3.1. Cumulative Total CO_2 Emissions and EOM-Derived Emissions

The addition of all EOMs resulted in a significant increase in cumulative CO_2-C emissions ($p < 0.05$) (Table 2). On day 92, the total CO_2-C emissions from the mesocosms were as follows, from lowest to highest: CL < SF < DG1 < DG2 = MN = MZ. Comparatively, the MZ treatment emitted sixteen times more CO_2 cumulatively than the CL soil, MN emitted twelve times, DG2 eleven, DG1 seven and SF four times the amount of the CL. Emissions from the MN and DG2 treatments amounted to 74 and 70%, respectively, of the total CO_2-C emissions from MZ (Table 2). The slopes of cumulative CO_2-C emission from DG1 and DG2 were very close until day 28, after which point, a sharp increase was observed for DG2 from day 37 to 48, followed by a slower increase up to day 92, by which time it had almost caught up with the MN treatment (Table 2 and Figure S1).

Table 2. Cumulative CO₂-C emissions after 92 days (mg CO₂-C kg^{−1} soil).

Parameter	CL	MZ	MN	SF	DG1	DG2
CO ₂ -C _{EOM}	/	901 ± 72 b	661 ± 167 ab	194 ± 36a	393 ± 26 ab	565 ± 46 ab
CO ₂ -C _{soil}	63 ± 11 ab	90 ± 10 ab	77 ± 4 ab	63 ± 23ab	51 ± 8 a	149 ± 29 b

CO₂-C_{EOM} = the cumulative CO₂-C derived from the EOM on day 92; CO₂-C_{soil} = the cumulative CO₂-C derived from the soil on day 92. MZ: maize; MN: manure; DG1 and DG2: digestate; SF: the solid fraction of digestate; CL: control soil with no addition of fertiliser. Treatments with the same letters are not statistically different ($p < 0.05$).

Emissions from the CL were on average 0.73 mg CO₂-C 24 h^{−1} over the course of the experiment and, on day 92, the cumulative CO₂-C had reached 63 mg kg^{−1} soil. After 48 h, MZ had rapidly set itself apart with 206 mg cumulative CO₂-C kg^{−1} soil, while MN reached 154 mg CO₂-C kg^{−1} soil. In contrast, DG1 and DG2 had emitted, respectively, 52 and 87 mg CO₂-C kg^{−1} soil. The SF was the lowest of all EOM treatments at 19 mg CO₂-C kg^{−1} soil, whereas the CL had reached a cumulative 3.29 mg CO₂-C kg^{−1} soil after 48 h.

The results of the EOM-derived cumulative CO₂-C emissions (Equation (1)) on day 92, expressed as a percentage of added TOC (TOC_{min-EOM}, Table 3), were as follows: 11%_{SF}~23%_{DG1}~35%_{DG2}~38%_{MN} < 50%_{MZ}. A second-order kinetic C model (Equation (4)) was fitted to the experimental data ($p < 0.0001$) and allowed to estimate the amount of remaining TOC after 1 to 2 years (TOC_{seq-EOM}, Table 3), which was considered as the sequestrable fraction. From highest to lowest, the TOC_{seq-EOM} from the EOMs was as follows: SF > DG1 > MN > DG2 > MZ. Regarding MZ, ranges of 50–60% of mineralised C derived from maize have been reported in year-long soil incubation experiments [36], which fall in line with the 56% of mineralised TOC from MZ after 1 year predicted using the second-order kinetic model. On the opposite side of the spectrum, TOC_{seq-EOM} from the SF was the highest at 86%, almost double the value of MZ. The SF was trailed by DG1 (Table 3). The second-order model indicated that CO₂-C from DG2 would have caught up with MN by day 221, the tipping point at which both EOMs would contain 59.1% of residual TOC. After this point, DG2 would overtake MN, as could be anticipated from the data trend (Figure 1a), and as confirmed by the final results of the model, which indicated 56 and 58% TOC_{seq-EOM}, respectively, for DG2 and MN (Table 3).

Table 3. Cumulative CO₂-C expressed in relation to total organic carbon applied (% TOC).

Parameter	MZ	MN	SF	DG1	DG2
TOC _{min-EOM}	50.5 ± 4.1 b	37.6 ± 9.5 ab	11.0 ± 2.1 a	23.2 ± 1.5 ab	34.6 ± 2.8 ab
TOC _{seq-EOM}	43.9	58.3	85.9	73.2	56.2

TOC_{min-EOM} = the percentage of mineralised total organic carbon derived from the added exogenous organic matter on day 92; TOC_{seq-EOM} = the percentage of remaining total organic carbon after 1 to 2 years calculated with the second-order kinetic model. MZ: maize; MN: manure; DG1 and DG2: digestate; SF: the solid fraction of digestate. Treatments with the same letters are not statistically different ($p < 0.05$).

For MZ, MN, DG1 and DG2, the EOM-derived CO₂-C emission was the highest on the first day with, respectively, 79.3; 56.3; 17.0 and 35.7 mg CO₂-C kg^{−1} soil 24 h^{−1} (Figure S2a). For SF, the peak came later, on day 9, with 6.6 mg CO₂-C kg^{−1} soil 24 h^{−1}. Once the peak had been reached (day 9 for SF and day 1 for other EOMs), the general trend was that of a decrease in the CO₂-C derived from EOM materials over time, as could be expected. However, in the case of DG2, as a departure from the blueprint described above, 2.5 mg CO₂-C kg^{−1} soil 24 h^{−1} were measured on day 28, after which a pulse was observed, reaching its peak on day 48 with 8.1 mg CO₂-C kg^{−1} soil 24 h^{−1}, followed by a progressive decline to eventually reach its lowest point by day 92 at 2.3 mg CO₂-C kg^{−1} soil 24 h^{−1} (Figure S2a). In spite of these pulses, all emissions gradually converged on the last day, ranging between 0.7 and 2.3 mg CO₂-C kg^{−1} soil 24 h^{−1} (against 0.67 mg for the CL). By that time, the values were no longer significantly different (Table S4).

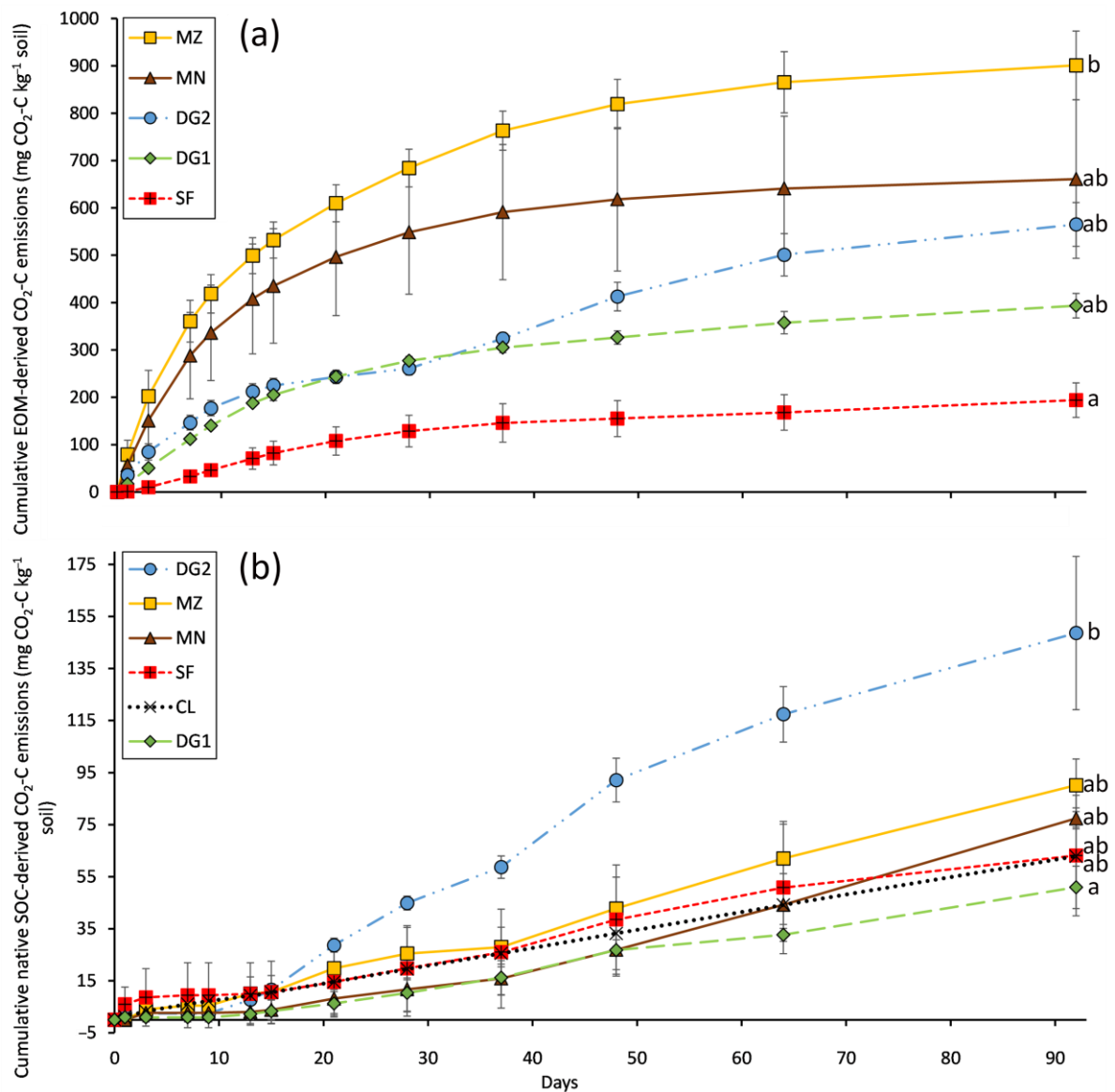


Figure 1. Evolution of the cumulative (a) EOM-derived CO₂-C and (b) native SOC-derived CO₂-C over 92 days. MZ: maize; MN: manure; DG1 and DG2: digestate; SF: the solid fraction of digestate; CL: control soil with no addition of fertiliser. Treatments with the same letters denote no statistical difference ($p < 0.05$) in the 92-day cumulative CO₂-C emissions.

3.2. Native SOC-Derived CO₂ Emissions and SOC Priming

The CL had emitted a cumulative 63 mg CO₂-C kg⁻¹ soil by day 92 (Table 2) with an average emission rate of 0.73 mg CO₂-C 24 h⁻¹, which was linear throughout. Expressed relatively, this corresponded to 4.3% of mineralised native SOC on day 92. On day 92, the differences in SOC-derived mg CO₂-C kg⁻¹ soil 24 h⁻¹ between treatments had become negligible (Table S4). The SF soil had the highest SOC-derived CO₂ emission rate during the first 9 days (Figure S2b). From day 28 onwards, the SF SOC-derived CO₂ emissions were closely aligned to those of the unamended CL soil, and no net cumulative SOC-derived emissions were observed on day 92 (Figure 1b), resulting in a cumulative PE (Equation (3)) of 0.5% relative the cumulative emissions from the CL soil, which was not significantly different. With MZ, SOC mineralisation surpassed that of the CL soil from day 13 onwards (Figure 1b) and, overall, although not significantly different, cumulative SOC-derived emissions were higher than the CL by 27 mg CO₂-C kg⁻¹ on day 92 (Table 2). The PE from MZ-SOC was 43% higher than the CL soil, which resulted in it being significantly

different ($p < 0.05$) (Figure 2). The mineralisation of the SOC-derived MN treatment was inferior to the CL until day 64 (Figure 1b), at which point the cumulative amount of SOC overtook that of the CL treatment to reach a net positive difference of $14 \text{ mg CO}_2\text{-C kg}^{-1}$ by day 92 (Table 2). The final cumulative PE from MN-SOC amounted to a significant difference of 23% compared with the CL soil (Figure 2). As for DG1, SOC-derived CO_2 emissions were lower than the CL treatment from the onset until the end (Figure S2b), and the cumulative SOC-derived emissions after 92 days were lower than the CL soil by $12 \text{ mg CO}_2\text{-C kg}^{-1}$ but not significantly different (Table 2, Figure 1b). The PE of DG1 was -19% , this result was not significantly different from the CL soil (value of 0) according to the *T*-test. In stark contrast, DG2 started off with a similar trend but set itself apart from day 13 onwards, showcasing the highest SOC-derived emissions (Table 2, Figure 1b) and the highest positive priming of all EOMs by the end of the experiment (Figure 2). By day 92, the two digestates thus delineated the two ends of the priming spectrum with a negative PE of -19% from DG1 and $+137\%$ from DG2 compared with the basal respiration of the CL (Figure 2). Overall, when comparing the EOMs against one another, the PEs (Equation (3)) were only significantly different ($p < 0.05$) between DG1 and DG2 (Figure 2): $-19\%_{\text{DG1}} \sim +0.5\%_{\text{SF}} = +23.2\%_{\text{MN}} = +43.4\%_{\text{MZ}} < +136\%_{\text{DG2}}$.

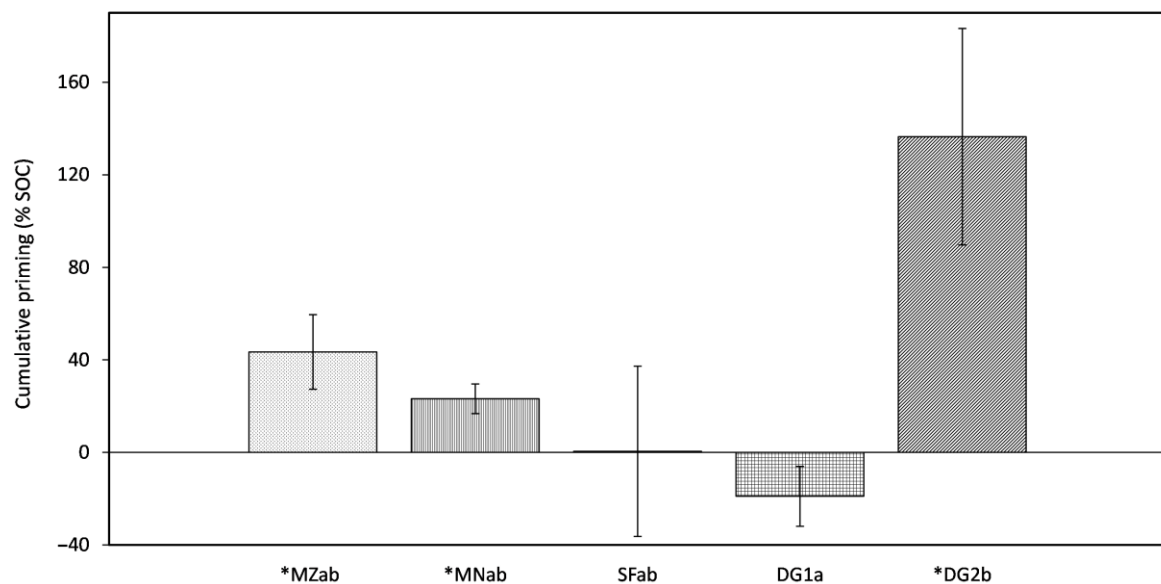


Figure 2. Cumulative priming after 92 days expressed in relation to the CO_2 emissions of the native soil organic carbon from the control soil (Equation (3)). MZ: maize; MN: manure; DG1 and DG2: digestate; SF: the solid fraction of digestate. Treatments with the same letters are not statistically different ($p < 0.05$) according to Tukey's HSD test. * Treatments that are statistically significantly different from the unamended control soil according to the *T*-test ($p < 0.05$).

3.3. Microbial Biomass Carbon

In the case of DG1 and DG2, the relative increase in MBC was not significantly different from the CL (Table 4). Compared with the 39 mg C kg^{-1} soil of the CL, the DG1 and DG2 EOMs had statistically similar effects in terms of MBC gains and were responsible for the lowest increase from the EOMs vs. CL, representing roughly a 60–65% increase (an additional 26 and 25 mg C kg^{-1} soil, respectively). The SF resulted in an additional 52 mg C kg^{-1} soil (or 133% increase), while MZ and MN led to the highest turnover with, respectively, an additional 87 and 67 mg C kg^{-1} soil (Table 4), which represented an increase of 223% for MZ and 172% for MN.

Table 4. Main results from post-incubation analyses carried out on soil cores on day 92.

Parameter	Unit	CL	MZ	MN	SF	DG1	DG2
pH _{KCl}	/	6.6c ± 0.0	6.8d ± 0.0	6.5bc ± 0.0	6.9e ± 0.0	6.4b ± 0.1	6.3a ± 0.1
MBC	mg C kg ^{−1} soil	39a ± 10	126c ± 9	106cd ± 22	91bc ± 11	65ab ± 23	64ab ± 10
Mineral N _{residual}	mg kg ^{−1} soil	28a ± 1	26a ± 1	99b ± 3	37c ± 2	136d ± 10	175e ± 11

MBC = microbial biomass carbon on day 92; Mineral N_{residual} = the residual mineral nitrogen in the soil cores calculated as the sum of NH₄⁺–N and NO₃[−]–N on day 92. MZ: maize; MN: manure; DG1 and DG2: digestate; SF: the solid fraction of digestate; CL: control soil with no addition of fertiliser. Treatments with the same letters are not statistically different ($p < 0.05$).

3.4. Residual Mineral N

With the exception of the CL and MZ mesocosms, some significant differences in recovered residual mineral N (defined as the sum of NH₄⁺–N and NO₃[−]–N at the end of the experiment) were observed between treatments ($p < 0.05$, Table 4). When considering the forms of N contained in the different EOMs at the onset of the experiment, MZ was the only one that already contained a small amount of 0.9 g NO₃[−]–N kg^{−1}, while it also contained an almost equivalent quantity of NH₄⁺–N of 1.1 g kg^{−1} (Table 5). It is a widely held view that digestate usually contains a higher ratio of NH₄⁺–N than undigested feedstocks [37,38], and this assumption was confirmed in this study (Table 5). It follows that the highest NH₄⁺–N-containing EOMs were DG2, DG1 and MN with, respectively, 39, 22 and 21 g NH₄⁺–N kg^{−1} (Table 5). The lower content of NH₄⁺–N (2.4 g kg^{−1}) in the SF of digestate was expected, as most of it would have volatilised during the drying/heating process that this EOM was subjected to (Section 1). Turning to the residual NH₄⁺–N in the amended mesocosm on day 92, trace amounts were found, which ranged from 0.39 (DG2) to 1.04 (MZ) mg NH₄⁺–N kg^{−1} soil (Table S6), and nearly all mineral N in the soil was in the form of NO₃[−]–N. Soil mineral N content at day 92 was as follows: MZ = CL < SF < MN < DG1 < DG2 (Table 4).

Table 5. Main physicochemical properties of the exogenous organic matter materials. Results are expressed on a dry matter basis.

Parameter	Unit	MZ	MN	SF	DG1	DG2
δ ¹³ C	(‰)	−12.9	−17.8	−14.4	−13.5	−13.7
pH _{KCl}	/	6.1 ± 0.0	8.5 ± 0.0	9.6 ± 0.0	8.1 ± 0.0	8.0 ± 0.0
EC	(mS cm ^{−1})	1.5 ± 0.0	3.9 ± 0.0	10.3 ± 0.0	4.1 ± 0.0	4.9 ± 0.0
TC	(g kg ^{−1})	408 ± 9	432 ± 14	420 ± 13	458 ± 21	365 ± 22
TOC	(g kg ^{−1})	408 ± 9	425 ± 13	414 ± 16	435 ± 22	334 ± 26
DOC	(g kg ^{−1})	143	154	32	231	129
TN	(g kg ^{−1})	20.8 ± 0.2	46.9 ± 3.6	33.3 ± 1.0	62.2 ± 2.7	81.1 ± 2.7
NH ₄ ⁺ –N	(g kg ^{−1})	1.1 ± 0.2	20.6 ± 0.1	2.4 ± 0.3	22.2 ± 0.2	38.8 ± 0.3
NO ₃ [−] –N	(g kg ^{−1})	0.9 ± 0.3	0.0 ± 0.0	0.0 ± 0.0	0.0 ± 0.0	0.0 ± 0.0
Lignin	(g kg ^{−1})	35	124	133	131	144
Cellulose	(g kg ^{−1})	235	291	162	186	274
C/N	/	19.6	9.2	12.6	7.4	4.5
DOC/TC	/	0.35	0.36	0.08	0.46	0.33
NH ₄ ⁺ –N/TN	/	0.05	0.44	0.07	0.36	0.48

MZ: maize; MN: manure; DG1 and DG2: digestate; SF: the solid fraction of digestate. δ¹³C = ¹³C isotope analysis of dry substrate; EC = electrical conductivity; TC = total carbon; TOC = total organic carbon; DOC = dissolved organic carbon; TN = total nitrogen; NH₄⁺–N = ammonium nitrogen; NO₃[−]–N = nitrate nitrogen

3.5. pH Measurements

Some slight shifts in pH were observed at the end of the experiment, revealing significant differences ($p < 0.05$) between some of the treatments (Table 4). Mesocosms that were amended with MN, DG1 and DG2 led to acidification compared with the CL, with pH values of 6.5, 6.3 and 6.4, respectively. In contrast, the MZ and SF EOMs induced an alkalisation of the soil with pH values of 6.8 and 6.9, respectively.

4. Discussion

4.1. Nitrogen Budget and Dynamics

During nitrification, two H^+ cations are generated with each newly formed $NO_3^- - N$ molecule. In a plant–soil system, along with the uptake of $NO_3^- - N$, the plant neutralises one of the two H^+ cations by releasing HCO_3^- . Under the controlled conditions of the present study, in the absence of plants, the generated H^+ ions were left unchecked, as a result of which, they accumulated as permanent soil acidity [39]. This explains the drop in pH observed with MN, DG1 and DG2—all $NH_4^+ - N$ -heavy EOMs—as a result of which, it is reasonable to assume that nitrification was the predominant biological driver behind the observed drop in $NH_4^+ - N$ and the concomitant increase in $NO_3^- - N$ [40]. Similar trends from nitrification-induced acidification have been reported [41], whereas the accumulation of organic acid intermediates and amino acids in digestate has also been put forward as a possible reason for the drop in pH [42]. Thus, the expected liming effect of the NH_4^+ -rich DG1 and DG2, owing to the presence of carbonates, was eclipsed by the acidification from the excess H^+ that was released upon nitrification, which the significantly negative relationships between pH KCl_{day92} and the mineral $N_{residual}$ ($p < 0.01$), on one part, and pH KCl_{day92} and the amount of added $NH_4^+ - N$ ($p < 0.05$), on the other, appeared to co-explain (Table S7).

As an indication of the mineral N released by EOMs, we compared the balance between the original inputs of $NH_4^+ - N$ from the MN, DG1 and DG2 materials (Table S5) and the residual mineral N extracted from the soil cores on day 92, after subtracting the amount of N mineralised in the CL (Table S6). In the case of MN, the initial input was on average 85 mg $NH_4^+ - N \text{ kg}^{-1}$ soil (Table S5) for 71 mg $NO_3^- - N \text{ kg}^{-1}$ extracted on day 92 (Table S6). For DG1, 87 mg $NH_4^+ - N \text{ kg}^{-1}$ soil was added and 109 mg $NO_3^- - N \text{ kg}^{-1}$ was retrieved on day 92, showcasing a surplus of 22 mg $NO_3^- - N$, which would attest to the mineralisation of the DG1 N_{org} pool and/or native SOM. For DG2, 190 mg $NH_4^+ - N \text{ kg}^{-1}$ soil was added and 147 mg $NO_3^- - N \text{ kg}^{-1}$ was extracted on day 92, leaving 43 mg or 23 % of the initial $NH_4^+ - N$ unaccounted for. This represented the highest apparent loss, followed by MN, for which a 14 mg $N \text{ kg}^{-1}$ deficit (17%) between the initial $NH_4^+ - N$ and recovered $NO_3^- - N$ was observed. In laboratory mesocosms, there are three principal pathways for losses of minerals: (1) net N-immobilisation into microbial biomass and thereafter into necromass, (2) denitrification losses and (3) NH_3 -volatilisation. Regarding immobilisation, by assuming an overall MBC/MBN ratio of 8.6 [43], we inferred the MBN based on the measured MBC results (Table 4). More specifically, the MBN for the two treatments that showcased an N-deficit, or apparent loss, would have been 12 and 7 mg MBN kg^{-1} soil for MN and DG2, respectively. It follows that the apparent loss of 14 mg $N \text{ kg}^{-1}$ from MN would have been largely offset by MBN immobilisation. For DG2, an estimated 7 mg of immobilised N would result in 36 mg of unaccounted N (or a 20% apparent loss). If reduction of NO_3^- had occurred, its effects would have been negligible under the predominantly aerobic conditions provided at 50% WFPS, which are highly supported by the observed nitrification. Thus, the apparent N loss from DG2 could be ascribed to volatilisation, which digestate has been shown to be prone to [44,45]. In effect, the unaccounted $NH_4^+ - N$ expressed over the amount of TN supplied by the DG2 EOM would result in a loss of 9%, which is in general accordance with the range of 15% reported by [12].

The MZ material was characterised by ratios of 0.94 N_{org}/TN , 0.35 DOC/TC and 19.6 C/N (Table 5). Therefore, MZ would have carried substantial amounts of labile C, increasing microbial demand for N, in which case, N mining could have occurred [46,47]. However, the residual mineral N on day 92 in the CL and MZ mesocosms were almost identical (Table 4), indicative of an equilibrium state between N mineralisation and immobilisation that is also typical for OM with a C/N ratio between 20 and 30 [48]. The SF product displayed an even higher N_{org}/TN ratio of 0.99, but a net positive balance of 9.8 mg mineral $N \text{ kg}^{-1}$ compared with the CL suggests that a slow net N mineralisation took place, probably favoured by a lower C/N ratio in comparison with MZ (Table 5).

4.2. EOM-C Mineralisation and Priming Effect

Looking at the physicochemical properties of the EOMs, the best predictors for EOM-C mineralisation were the contents of lignin, for which a marginally negative correlation was established, and cellulose, for which a marginally positive relationship was established (Table S7). Hence, the recalcitrance of lignin to biological degradation was partly reflected in this study ($p < 0.05$, Table S7). A similar negative relationship was reported between the mineralised C and the lignin content in incubation experiments with digestates and manures [49]. The only study to our knowledge that used the natural ^{13}C abundance tracer technique with a focus on digestate reported 63% C sequestration from digested maize after a 178-day incubation [50], whereas we found 60% and 75% of stored C (Figure 3) from DG2 and DG1, respectively, in this study. So, while at least for one of the studied digestates, the reported sequestration range was similar, it also highlights that when studying several digestates, the range of results can be quite different, which points to the heterogeneity in such products.

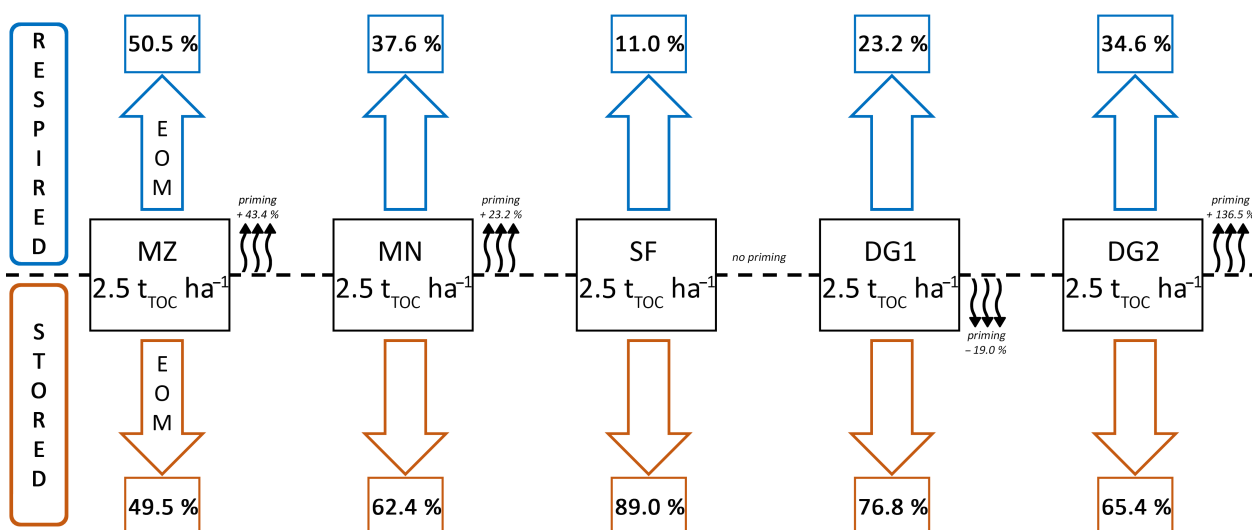


Figure 3. TOC budget from the EOMs at the end of the experiment resulting from the addition of $2.5 \text{ t TOC ha}^{-1}$. The upper half (above the dotted line) shows the fraction of mineralised (respired) TOC, the lower half (below the dotted line) shows the amount of unmineralised (stored) TOC that still remained after 92 days. The fractions of TOC (respired and stored) are expressed as a percentage of TOC applied and in resulting tonnes of TOC ha^{-1} . The priming percentages are for additional illustrative purposes, they show the amount of CO_2 emitted relative to the unfertilised control soil. MZ: maize; MN: manure; DG1 and DG2: digestate; SF: the solid fraction of digestate.

In terms of PE, the only two treatments that were significantly different were DG1, associated with negative priming, and DG2, associated with the highest positive priming ($p < 0.05$, Figure 2). The three remaining treatments, namely, MZ, MN and SF, fell somewhere in between and were not significantly different to either DG1 or DG2. The SF provided comparable amounts of mineral N to the MZ treatment (Table S5), whereas no PE was observable on the last day of the experiment. It can be assumed that the higher amount of stabilised C from the SF—which supplied the lowest quantities of DOC—meant that little energy was available for soil microorganisms; hence, its addition to the soil elicited a low microbial response [24] probably dominated by k-strategists [51]. Similar trends in increased MBC from soils amended with SF were also observed by [52], who also reported a significant increase in the fungi-to-bacteria ratio as a probable reaction to the higher concentrations of lignified compounds contained in the SF. With the highest MBC of the three digestates, it can be hypothesised that the SF is prone to leave behind higher amounts of necromass, which has been shown to be the primary precursor of stable soil organic matter [53].

Ref. [54] proposed that the amount of easily available OC added could influence the direction of priming to the effect that exogenous C exceeding 200–500% of the MBC could result in a neutral or negative PE. Considering that the initial MBC usually does not exceed 5% TOC [55,56], a conservative value of 2% was used, resulting in an estimated initial amount of 117 mg MBC kg^{−1} soil. Accordingly, quantities of added DOC, taken as the most easily degradable fraction of C, were calculated as a percentage of the initial MBC. The ratios of DOC to MBC were as follows: 530%_{MZ}; 544%_{MN}; 117%_{SF}; 768%_{DG1}; 537%_{DG2}. In other words, with the exception of the SF, all treatments were in the 200–500% range or beyond. While the thresholds in the present study did not quite match the theorised blueprint [54], it could be noted that DG1, the only treatment behind negative priming, provided the highest amounts of DOC alongside easily accessible NH₄⁺–N. According to the ‘preferential substrate theory’, the addition of a substantial quantity of easily degradable C alongside mineral N would have induced microbes to shift from the SOC to the DG1 substrate as a primary source to acquire energy (C) and nutrients (N) [57,58] as a consequence of which, mineralisation of the native SOC would be lower than in the control soil. On the same topic, [59] reported neutral and negative priming linked to preferential substrate utilisation after applying a high rate of glucose corresponding to 8 times the amount of the MBC in the soil (compared with 7.7 times in the case of DG1) with high N supplementation. The authors proposed that under such conditions of easily accessible C and N in excess, competition between r- and k-strategists is negligible, while k-strategists—typically associated with SOM decomposition—would switch to these readily available sources. Along this line of thought, DG1 provided the largest amount of DOC (Table 4) and a high supply of mineral N, and thus, the microbial community would have switched its uptake to the large DOC pool supplied by DG1.

In one of the very few studies that used the natural ¹³C abundance tracer technique to infer PE using digestate [50], the PE from digestate and maize treatments were measured at −18% and +57%, respectively, which generally match the direction and intensity of some of the observed PE in this study (−19% for DG1 and +43% for MZ). The authors ascribed the negative PE of their digestate treatment to a probable higher presence of aliphatic molecules [60] and other complex aromatic compounds derived from lignin materials [61], which are recalcitrant fractions usually found in higher concentrations in digested, rather than undigested, feedstocks [62]. It is also worth noting that the presence of such C compounds in digestate (identified using spectroscopic analysis in the studies referenced above) tends to vary according to specific digestion parameters. In this light, the contrasting hydraulic retention times, 29 days for DG1 and 72 days for DG2, and the different AD processes, two-stage digestion for DG1 and one-stage for DG2 (Section 2.1), could have had an impact on the macromolecular composition and concentrations of such recalcitrant compounds and therefore might also have played a part in the highly contrasted PE of DG1 (−19%) and DG2 (+136%).

In the case of DG2, another possible priming mechanism might have been at play. Indeed, almost half of the N it contained was in the form of NH₄⁺–N, while its low C/N ratio (Table 4) meant that the added C carried close to 400 mg TN kg^{−1} soil, of which 190 mg NH₄⁺–N kg^{−1} soil represented more than double the second highest treatment (Table S5). Ref. [63] found that the addition of NH₄⁺–N at a rate of 200 mg kg^{−1} enhanced the decomposition of native SOM three- to fourfold in different soils treated with glucose and maize after 28 days. In this study, the PE from DG2 was 2.4 times that of the CL (Figure S2b) with 190 mg NH₄⁺–N kg^{−1} supplied by the EOM. Therefore, the profusion of NH₄⁺–N might have driven microorganisms to switch to native recalcitrant SOC for metabolic needs since easily accessible N was not a limiting factor, as suggested by [63].

At any rate, the current theoretical frameworks and proposed mechanisms to explain soil priming remain somewhat controversial [54,64] and can lead to seemingly contradictory results. The linear relationship between the input of labile C and the magnitude and direction of priming has been found to be positive in some instances [65] and negative in others [66], whereas both negative and positive priming were observed in the presence

of added labile C in this study. This can also be the consequence of the theorised underlying mechanisms occurring simultaneously [57,67]. To summarise, it appears that the initial addition of MN, DG1 and DG2 supplied labile C in excess of the MBC, alongside non-limiting provisions of N at the beginning, which appear to have triggered an initial negative PE (Figure S2b) as SOM decomposers turned preferentially to the labile EOM-C. A posteriori, it can be hypothesised that the main difference in the observed cumulative PE was probably that the pool of labile C became depleted before the available N in the case of DG2 and MN treatments; hence, the fresh EOM decomposers switched, in those cases, to SOM [68]. To elucidate the underlying mechanisms that were at play, an analysis of soil enzyme activity, which goes beyond the scope of this study, might have been instrumental in identifying the active microbial community structures in the different treatments.

4.3. C Input from Digestates and Agronomic Implications

The soil C cycle is a dynamic balance between C inputs (litter, photosynthesis) and outputs (decomposition, erosion and leaching mechanisms) [69]. Globally, soil is the largest terrestrial pool of OC holding an estimated 1500 Pg in the first 100 cm [70]. Should it switch from sink to source (increased CO₂ emissions into the atmosphere); a small change in this large pool could lead to a C cycle feedback loop that could significantly accelerate climate change [71]. Projected changes in SOC rely on a complex mosaic of regional parameters (temperature, rainfall, moisture, soil type, land use, changes in net primary production) and a sensitive balance between C losses and gains [72,73].

Regional specificities aside, cropland is seen as the largest actionable sink for C sequestration [70,74] in view of the fact that it is already under active management (no land use change strategy required) and is typically already C-depleted [75]. Under this scenario, the addition of the digestate EOMs—DG1, DG2 and SF—would yield high fractions of remaining particulate C (Figure 3). To further home in on the estimated portion of soil-sequestrable OC, the second-order kinetic model (Equation (4)) allowed us to estimate the unmineralised fraction after 1 to 2 years (TOC_{seq-EOM}, Table 3) with a high degree of confidence ($p < 0.0001$). With 86 and 73% of TOC_{seq-EOM}, respectively, the SF and DG1 demonstrated the highest C potentials for sequestration, corresponding to 2.2 and 1.8 t TOC ha⁻¹, respectively, when added at 2.5 t OC ha⁻¹.

To increase SOC, a multi-dimensional approach is usually recommended that includes management practices such as reduced or no tillage, the use of cover and catch crops, the input of organic materials, the integration of crop rotations [76], the inclusion of field margins, buffer strips and hedgerows [77]. Drawing attention to the inputs, a recent study highlighted that under the current levels of OC inputs to German croplands, the modelled SOC would drop by a staggering 10 to 18% by the end of the 21st century [78]. They further stated that to counterbalance the climate change-induced losses and maintain the current SOC levels, predicted OC inputs would need to increase by as much as 51 to 93% (1.3 to 2.3 t OC ha⁻¹ y⁻¹) [78]. With this in mind, the studied digestates would make for interesting C inputs with additional C ranging from 1.6 to 2.2 t OC ha⁻¹ (Figure 3). Nevertheless, this potential for SOC build-up must be nuanced to some extent. In the present study, an equal share of C at a rate of 2.5 t TOC ha⁻¹ was used (Section 2.1). In this circumstance, the amount of N applied with each treatment was at times widely different as a result of the varying C/N properties of each EOM (Table 4). In practice, the 2.5 t TOC ha⁻¹ carried an associated 199 and 339 kg N ha⁻¹ in the cases of SF and DG1, respectively, and a soaring 556 kg N ha⁻¹ for DG2. In other words, these N regimes are not directly transferable to field conditions. In the frame of the Nitrates Directive (91/676/EEC), to protect surface waters and groundwater from nutrient pollution arising from agricultural sources, N from animal manure is limited to 170 kg N ha⁻¹ y⁻¹ in nitrate vulnerable zones (NVZs), whereas in certain regions such as Flanders, it represents the limit by default. Of course, this provision extends to the use of digestates (or other products) that contain manure of animal origin as feedstock [79]. While the digestates in this study were elaborated from maize and,

therefore, technically do not contain any materials of animal origin, the associated N values mentioned above call for caution at the very least.

In most cases, the use of digestates (and other organic inputs such as animal manure) will require specific checkmarks, which can somewhat limit the room for manoeuvre in spite of an interesting potential in terms of C input. Continuing with the example of Belgium, agricultural land (including permanent grassland) covers approximately 1.36 million ha, with croplands accounting for approximately 63% [80]. From 1960 to 2006, high soil C gains were secured in the sandy croplands of Flanders, stemming from the liberal use of manure in these livestock-intensive regions until 1990 [81], that is, until the implementation of the Nitrates Directive. Nowadays, most agricultural soils in Flanders are nutrient-rich and exhibit surpluses of N and P, whose origins can in most cases be traced back to intensive livestock husbandry activities [82,83]. On the other hand, in recent decades, C levels in croplands along the loess belt, which sits across the regions of Flanders and Wallonia, have dropped critically to less than 1%. This situation has led to a decline in soil aggregate stability and has left those soils vulnerable to surface crusting and muddy floods after heavy rainfall [84,85]. This area, which covers roughly a third (0.26 million ha) of Belgian croplands, has been pinpointed as having the greatest potential for C sequestration, while, on average, a value of $0.88 \text{ t C ha}^{-1} \text{ year}^{-1}$ has been put forward to achieve a 4 per 1000 increase in topsoil (0–30 cm) sequestration in Belgian croplands [85]. Thus, while in principle this target could be met using digestate-mediated solutions (Figure 3), an important caveat is that it can only be performed proportionally to the amount of nutrients (N, P) that these C-impovertised soils can take on. In this respect, if we zoom out and consider the European landscape as a whole, NVZs cover approximately 61% of agricultural areas [86]. This state of affairs imposes a predominantly nutrient-driven rationale, implying, as a corollary, that the C-input from digestate will logically take a back seat in the face of water quality imperatives delineated in the Nitrates Directive.

Irrespective of the fertilisation strategies and the understandable focus on responsible nutrient stewardship and budgeting, SOC loss is of increasing concern [75]. While these two facets have no reason to be mutually exclusive, in the case of digestate (and manure), more often than not, the margin of action will be defined by a soil's pre-existing nutrient balance. Globally, there is an estimated 4900 Mha of agricultural land where SOC sequestration is feasible and where an increased input of EOM-C is needed to outweigh SOC losses from erosion and mineralisation [87]. That is to say, the field of action is wide, but as is normal practice, digestate is used primarily for its N-fertilising properties, and the nutrients it contains tend to restrict its scope of application as an input of C, expressly in 'nutrient hotspots'. In return, soils that are capable of accommodating a higher load of nutrients from digestate will reap maximum benefits also in terms of added C. Hence, its higher load of nutrients in relation to C makes digestate a fertiliser with C-loss compensating properties, rather than a C-centred amendment. By focusing on C dynamics, the present study has the merit of highlighting tangible collateral benefits, in terms of C input to the soil, that digestate can impart. In line with the observations made by [88] in a 3-year field experiment, we can conclude that even under nutrient-restrictive conditions (e.g., the Nitrates Directive in the European context), the application of digestate would be suitable to compensate C losses over time while maintaining crop productivity via its N-fertilising attributes.

5. Conclusions

At an application rate of 2.5 t OC ha^{-1} equivalent, 11% (SF), 23% (DG1) and 35% (DG2) of the applied OC from the digestates was mineralised after 92 days, against 50% for maize and 38% for cattle manure, showcasing an overall higher stability for digestates. The two liquid digestates (DG1 and DG2) had a sequestration potential of 56 and 73%, respectively, of the total applied OC after 1 to 2 years in comparison with 50% from maize. For the solid fraction of digestate (SF), this potential reached 86%. From an agronomic perspective, the use of digestate to increase OC input to soil can be considered as a secondary benefit after its main asset as an N fertiliser. Over a period of 92 days, in comparison with the

control soil, the PE of DG1 was negative (−19%) and the SF had no effect (0%), while DG2 exhibited positive priming (+136%), overall displaying a surprisingly contrasting range of microbial responses to the different digestate qualities.

Supplementary Materials: The following supporting information can be downloaded at: <https://www.mdpi.com/article/10.3390/agronomy13102501/s1>, Figure S1: Evolution of the total cumulative CO₂-C from the soil treatments over 92 days; Figure S2: Emissions from (a) the EOM-derived CO₂-C and (b) SOC-derived CO₂-C expressed as mg CO₂-C kg^{−1} soil 24 h^{−1} over 92 days; Table S1: Additional soil physicochemical properties; Table S2: Additional physicochemical properties of the exogenous organic matter materials; Table S3: Main parameters of the 2nd order kinetic model; Table S4: Exogenous organic matter and soil-derived CO₂-C on last day (92) expressed as mg CO₂-C kg^{−1} soil 24 h^{−1}; Table S5: Amounts of N added with each treatment on first day of experiment; Table S6: Amounts of residual N measured in the soil cores on last day of experiment; Table S7: Main results of Pearson's correlations.

Author Contributions: G.R.: Conceptualisation, data curation, formal analysis, investigation, methodology, visualisation, writing—original draft and writing—review and editing. S.S.: conceptualisation, methodology, supervision, validation, resources and writing—review and editing. H.L.: methodology and writing—review and editing. H.D.: project administration, resources and funding acquisition. I.S.: writing—review and editing. E.M.: funding acquisition, project administration, resources, supervision and writing—review and editing. All authors have read and agreed to the published version of this manuscript.

Funding: This work was supported by the European Union's Horizon 2020 Research and Innovation Programme under project NUTRI2CYCLE (grant agreement No 773682, 2018).

Data Availability Statement: Data will be made available on request.

Acknowledgments: We would like to thank Mitja Stürwold (Neuried biogas plant), David Wilken (BGK-Bundesgütegemeinschaft Kompost e.V.), Benoit Verrielle (Avenir Conseil Elevage), Gervais Deschodt, Eddy Decaestecker (Inagro), Sander Vandendriessche (Inagro), Ana Robles Aguilar (UGent/IRTA) and Andreas Dering (ADRW NaturPower GmbH) for their invaluable role in the sourcing and procurement of the organic materials needed for this study. Thank you to Eva-Maria Roth (University of Helsinki) and Angela Martín Vivanco (University of Helsinki) for facilitating effective communication with German stakeholders. We also extend our gratitude to Jan de Lille, Marie-Chantal Herteleer, Joachim Neri, Tina Coddens, Sophie Schepens, Mathieu Schatteman and Katja Van Nieuland for their decisive help with the physicochemical analyses. The technical expertise and assistance of Orly Mendoza was especially appreciated.

Conflicts of Interest: The authors declare that they have no known competing financial interest or personal relationship that could have appeared to influence the work reported in this paper.

References

1. Pivato, A.; Vanin, S.; Raga, R.; Lavagnolo, M.C.; Barausse, A.; Rieple, A.; Laurent, A.; Cossu, R. Use of digestate from a decentralized on-farm biogas plant as fertilizer in soils: An ecotoxicological study for future indicators in risk and life cycle assessment. *Waste Manag.* **2016**, *49*, 378–389. [CrossRef]
2. Głowacka, A.; Szostak, B.; Klebaniuk, R. Effect of Biogas Digestate and Mineral Fertilisation on the Soil Properties and Yield and Nutritional Value of Switchgrass Forage. *Agronomy* **2020**, *10*, 490. [CrossRef]
3. Peng, W.; Pivato, A. Sustainable Management of Digestate from the Organic Fraction of Municipal Solid Waste and Food Waste Under the Concepts of Back to Earth Alternatives and Circular Economy. *Waste Biomass Valorization* **2017**, *10*, 465–481. [CrossRef]
4. O'Shea, R.; Lin, R.; Wall, D.M.; Browne, J.D.; Murphy, J.D. A comparison of digestate management options at a large anaerobic digestion plant. *J. Environ. Manag.* **2022**, *317*, 115312. [CrossRef] [PubMed]
5. Malhotra, M.; Aboudi, K.; Pisharody, L.; Singh, A.; Banu, J.R.; Bhatia, S.K.; Varjani, S.; Kumar, S.; González-Fernández, C.; Kumar, S.; et al. Biorefinery of anaerobic digestate in a circular bioeconomy: Opportunities, challenges and perspectives. *Renew. Sustain. Energy Rev.* **2022**, *166*, 112642. [CrossRef]
6. Vaneeckhaute, C.; Lebuf, V.; Michels, E.; Belia, E.; Vanrolleghem, P.A.; Tack, F.M.G.; Meers, E. Nutrient Recovery from Digestate: Systematic Technology Review and Product Classification. *Waste Biomass Valorization* **2017**, *8*, 21–40. [CrossRef]
7. Guilayn, F.; Rouez, M.; Crest, M.; Patureau, D.; Jimenez, J. Valorization of digestates from urban or centralized biogas plants: A critical review. *Rev. Environ. Sci. Bio/Technol.* **2020**, *19*, 419–462. [CrossRef]

8. Petraityte, D.; Arlauskienė, A.; Ceseviciene, J. Use of Digestate as an Alternative to Mineral Fertilizer: Effects on Soil Mineral Nitrogen and Winter Wheat Nitrogen Accumulation in Clay Loam. *Agronomy* **2022**, *12*, 402. [\[CrossRef\]](#)
9. Sigurnjak, I.; De Waele, J.; Michels, E.; Tack, F.M.G.; Meers, E.; De Neve, S. Nitrogen release and mineralization potential of derivatives from nutrient recovery processes as substitutes for fossil fuel-based nitrogen fertilizers. *Soil Use Manag.* **2017**, *33*, 437–446. [\[CrossRef\]](#)
10. Doyeni, M.O.; Stulpinaite, U.; Baksinskaite, A.; Suproniene, S.; Tilvikiene, V. The Effectiveness of Digestate Use for Fertilization in an Agricultural Cropping System. *Plants* **2021**, *10*, 1734. [\[CrossRef\]](#)
11. Lal, R. Food security impacts of the “4 per Thousand” initiative. *Geoderma* **2020**, *374*, 114427. [\[CrossRef\]](#)
12. Nkoa, R. Agricultural benefits and environmental risks of soil fertilization with anaerobic digestates: A review. *Agron. Sustain. Dev.* **2014**, *34*, 473–492. [\[CrossRef\]](#)
13. Nyang’Au, J.O.; Møller, H.B.; Sørensen, P. Nitrogen dynamics and carbon sequestration in soil following application of digestates from one- and two-step anaerobic digestion. *Sci. Total. Environ.* **2022**, *851*, 158177. [\[CrossRef\]](#)
14. Häfner, F.; Hartung, J.; Möller, K. Digestate Composition Affecting N Fertiliser Value and C Mineralisation. *Waste Biomass Valorization* **2022**, *13*, 3445–3462. [\[CrossRef\]](#)
15. Tambone, F.; Genevini, P.; D’imporzano, G.; Adani, F. Assessing amendment properties of digestate by studying the organic matter composition and the degree of biological stability during the anaerobic digestion of the organic fraction of MSW. *Bioresour. Technol.* **2009**, *100*, 3140–3142. [\[CrossRef\]](#)
16. Pognani, M.; D’imporzano, G.; Scaglia, B.; Adani, F. Substituting energy crops with organic fraction of municipal solid waste for biogas production at farm level: A full-scale plant study. *Process. Biochem.* **2009**, *44*, 817–821. [\[CrossRef\]](#)
17. Piccoli, I.; Francioso, O.; Camarotto, C.; Vedove, G.D.; Lazzaro, B.; Giandon, P.; Morari, F. Assessment of the Short-Term Impact of Anaerobic Digestate on Soil C Stock and CO₂ Emissions in Shallow Water Table Conditions. *Agronomy* **2022**, *12*, 504. [\[CrossRef\]](#)
18. Thomsen, I.K.; Olesen, J.E.; Møller, H.B.; Sørensen, P.; Christensen, B.T. Carbon dynamics and retention in soil after anaerobic digestion of dairy cattle feed and faeces. *Soil Biol. Biochem.* **2013**, *58*, 82–87. [\[CrossRef\]](#)
19. Leno, N.; Ajayan, A.S.; Thampatti, K.C.M.; Sudharmaidevi, C.R.; Aparna, B.; Gladis, R.; Rani, T.S.; Joseph, B.; Meera, A.V.; Nagula, S. Humification evaluation and carbon recalcitrance of a rapid thermochemical digestate fertiliser from degradable solid waste for climate change mitigation in the tropics. *Sci. Total. Environ.* **2022**, *849*, 157752. [\[CrossRef\]](#)
20. Slepėtienė, A.; Kochiieru, M.; Jurgutis, L.; Mankeviciene, A.; Skersiene, A.; Belova, O. The Effect of Anaerobic Digestate on the Soil Organic Carbon and Humified Carbon Fractions in Different Land-Use Systems in Lithuania. *Land* **2022**, *11*, 133. [\[CrossRef\]](#)
21. Reuland, G.; Sigurnjak, I.; Dekker, H.; Sleutel, S.; Meers, E. Assessment of the Carbon and Nitrogen Mineralisation of Digestates Elaborated from Distinct Feedstock Profiles. *Agronomy* **2022**, *12*, 456. [\[CrossRef\]](#)
22. Barlóg, P.; Hlisnikovský, L.; Kunzová, E. Effect of Digestate on Soil Organic Carbon and Plant-Available Nutrient Content Compared to Cattle Slurry and Mineral Fertilization. *Agronomy* **2020**, *10*, 379. [\[CrossRef\]](#)
23. Bastida, F.; García, C.; Fierer, N.; Eldridge, D.J.; Bowker, M.A.; Abades, S.; Alfaro, F.D.; Berhe, A.A.; Cutler, N.A.; Gallardo, A.; et al. Global ecological predictors of the soil priming effect. *Nat. Commun.* **2019**, *10*, 1–9. [\[CrossRef\]](#) [\[PubMed\]](#)
24. Fontaine, S.; Mariotti, A.; Abbadie, L. The priming effect of organic matter: A question of microbial competition? *Soil Biol. Biochem.* **2003**, *35*, 837–843. [\[CrossRef\]](#)
25. Li, H.; Bulcke, J.V.D.; Wang, X.; Gebremikael, M.T.; Hagan, J.; De Neve, S.; Sleutel, S. Soil texture strongly controls exogenous organic matter mineralization indirectly via moisture upon progressive drying—Evidence from incubation experiments. *Soil Biol. Biochem.* **2020**, *151*, 108051. [\[CrossRef\]](#)
26. Li, H.; Bulcke, J.V.D.; Kibler, P.; Mendoza, O.; De Neve, S.; Sleutel, S. Soil textural control on moisture distribution at the microscale and its effect on added particulate organic matter mineralization. *Soil Biol. Biochem.* **2022**, *172*, 108777. [\[CrossRef\]](#)
27. Keeling, D. Geochimica et Cosmochimica Acta 1958 Keeling. *Geochim. Cosmochim. Acta* **1958**, *13*, 1–13.
28. de Rooij, G.H. Methods of Soil Analysis. Part 4. Physical Methods. *Vadose Zone J.* **2004**, *3*, 722–723. [\[CrossRef\]](#)
29. Vance, E.D.; Brookes, P.C.; Jenkinson, D.S. An extraction method for measuring soil microbial biomass C. *Soil Biol. Biochem.* **1987**, *19*, 703–707. [\[CrossRef\]](#)
30. Joergensen, R.G.; Wu, J.; Brookes, P.C. Measuring soil microbial biomass using an automated procedure. *Soil Biol. Biochem.* **2011**, *43*, 873–876. [\[CrossRef\]](#)
31. Macherey-Nagel GmbH & Co. KG. “REF 985 825.”. Available online: <https://vendart.com.au/app/uploads/2019/10/985093-INSTRUCTIONS.pdf> (accessed on 26 September 2023).
32. Van Soest, P.J.; Robertson, J.B.; Lewis, B.A. Methods for dietary fiber, neutral detergent fiber, and nonstarch polysaccharides in relation to animal nutrition. *J. Dairy Sci.* **1991**, *74*, 3583–3597. [\[CrossRef\]](#) [\[PubMed\]](#)
33. Wordell-Dietrich, P.; Don, A.; Helfrich, M. Controlling factors for the stability of subsoil carbon in a Dystric Cambisol. *Geoderma* **2017**, *304*, 40–48. [\[CrossRef\]](#)
34. Thiessen, S.; Gleixner, G.; Wutzler, T.; Reichstein, M. Both priming and temperature sensitivity of soil organic matter decomposition depend on microbial biomass—An incubation study. *Soil Biol. Biochem.* **2013**, *57*, 739–748. [\[CrossRef\]](#)
35. Sleutel, S.; De Neve, S.; Roibas, M.R.P.; Hofman, G. The influence of model type and incubation time on the estimation of stable organic carbon in organic materials. *Eur. J. Soil Sci.* **2005**, *56*, 505–514. [\[CrossRef\]](#)
36. Stemmer, M.; Von Lützow, M.; Kandeler, E.; Pichlmayer, F.; Gerzabek, M.H. The effect of maize straw placement on mineralization of C and N in soil particle size fractions. *Eur. J. Soil Sci.* **1999**, *50*, 73–85. [\[CrossRef\]](#)

37. Möller, K.; Müller, T. Effects of anaerobic digestion on digestate nutrient availability and crop growth: A review. *Eng. Life Sci.* **2012**, *12*, 242–257. [\[CrossRef\]](#)
38. Cavalli, D.; Corti, M.; Baronchelli, D.; Bechini, L.; Marino Gallina, P. CO₂ emissions and mineral nitrogen dynamics following application to soil of undigested liquid cattle manure and digestates. *Geoderma* **2017**, *308*, 26–35. [\[CrossRef\]](#)
39. Bolan, N.S.; Hedley, M.J.; White, R.E. Processes of soil acidification during nitrogen cycling with emphasis on legume based pastures. *Plant Soil* **1991**, *134*, 53–63. [\[CrossRef\]](#)
40. Botheju, D.; Svalheim, O.; Bakke, R. Digestate Nitrification for Nutrient Recovery. *Open Waste Manag. J.* **2010**, *3*, 1–12. [\[CrossRef\]](#)
41. Zhao, X.; Wang, S.; Xing, G. Nitrification, acidification, and nitrogen leaching from subtropical cropland soils as affected by rice straw-based biochar: Laboratory incubation and column leaching studies. *J. Soils Sediments* **2013**, *14*, 471–482. [\[CrossRef\]](#)
42. Vaish, B.; Srivastava, V.; Singh, U.K.; Gupta, S.K.; Chauhan, P.S.; Kothari, R.; Singh, R.P. Explicating the fertilizer potential of anaerobic digestate: Effect on soil nutrient profile and growth of *Solanum melongena* L. *Environ. Technol. Innov.* **2022**, *27*, 102471. [\[CrossRef\]](#)
43. Cleveland, C.C.; Liptzin, D. C:N:P stoichiometry in soil: Is there a “Redfield ratio” for the microbial biomass? *Biogeochemistry* **2007**, *85*, 235–252. [\[CrossRef\]](#)
44. Wester-Larsen, L.; Müller-Stöver, D.S.; Salo, T.; Jensen, L.S.S. Potential Ammonia Volatilization from 39 Different Novel Biobased Fertilizers Applied to Soil—A Laboratory Study Using European Soils. *SSRN Electron. J.* **2022**, *323*, 1–30. [\[CrossRef\]](#)
45. Ni, K.; Pacholski, A.; Gericke, D.; Kage, H. Analysis of ammonia losses after field application of biogas slurries by an empirical model. *J. Plant Nutr. Soil Sci.* **2012**, *175*, 253–264. [\[CrossRef\]](#)
46. Webb, J.; Sørensen, P.; Velthof, G.; Amon, B.; Pinto, M.; Rodhe, L.; Salomon, E.; Hutchings, N.; Burczyk, P.; Reid, J. An Assessment of the Variation of Manure Nitrogen Efficiency throughout Europe and an Appraisal of Means to Increase Manure-N Efficiency. In *Advances in Agronomy*; Elsevier: Amsterdam, The Netherlands, 2013; Volume 119, pp. 371–442.
47. Moorhead, D.L.; Sinsabaugh, R.L. A theoretical model of litter decay and microbial interaction. *Ecol. Monogr.* **2006**, *76*, 151–174. [\[CrossRef\]](#)
48. Brust, G.E. *Management Strategies for Organic Vegetable Fertility*; Elsevier Inc.: Amsterdam, The Netherlands, 2019. [\[CrossRef\]](#)
49. Nielsen, K.; Roß, C.-L.; Hoffmann, M.; Muskulus, A.; Ellmer, F.; Kautz, T. The Chemical Composition of Biogas Digestates Determines Their Effect on Soil Microbial Activity. *Agriculture* **2020**, *10*, 244. [\[CrossRef\]](#)
50. Béghin-Tanneau, R.; Guérin, F.; Guiesse, M.; Kleiber, D.; Scheiner, J. Carbon sequestration in soil amended with anaerobic digested matter. *Soil Tillage Res.* **2019**, *192*, 87–94. [\[CrossRef\]](#)
51. Geyer, K.M.; Kyker-Snowman, E.; Grandy, A.S.; Frey, S.D. Microbial carbon use efficiency: Accounting for population, community, and ecosystem-scale controls over the fate of metabolized organic matter. *Biogeochemistry* **2016**, *127*, 173–188. [\[CrossRef\]](#)
52. Cattin, M.; Semple, K.T.; Stutter, M.; Romano, G.; Lag-Brotons, A.J.; Parry, C.; Surridge, B.W.J. Changes in microbial utilization and fate of soil carbon following the addition of different fractions of anaerobic digestate to soils. *Eur. J. Soil Sci.* **2020**, *72*, 2398–2413. [\[CrossRef\]](#)
53. Liang, C.; Schimel, J.P.; Jastrow, J.D. The importance of anabolism in microbial control over soil carbon storage. *Nat. Microbiol.* **2017**, *2*, 17105. [\[CrossRef\]](#)
54. Blagodatskaya, E.; Kuzyakov, Y. Mechanisms of real and apparent priming effects and their dependence on soil microbial biomass and community structure: Critical review. *Biol. Fertil. Soils* **2008**, *45*, 115–131. [\[CrossRef\]](#)
55. Lepcha, N.T.; Devi, N.B. Effect of land use, season, and soil depth on soil microbial biomass carbon of Eastern Himalayas. *Ecol. Process.* **2020**, *9*, 1–14. [\[CrossRef\]](#)
56. Anderson, T.-H.; Domsch, K. Ratios of microbial biomass carbon to total organic carbon in arable soils. *Soil Biol. Biochem.* **1989**, *21*, 471–479. [\[CrossRef\]](#)
57. Cheng, W. Rhizosphere feedbacks in elevated CO₂. *Tree Physiol.* **1999**, *19*, 313–320. [\[CrossRef\]](#)
58. Wang, H.; Boutton, T.W.; Xu, W.; Hu, G.; Jiang, P.; Bai, E. Quality of fresh organic matter affects priming of soil organic matter and substrate utilization patterns of microbes. *Sci. Rep.* **2014**, *5*, 10102. [\[CrossRef\]](#)
59. Blagodatskaya, E.; Blagodatsky, S.; Anderson, T.-H.; Kuzyakov, Y. Priming effects in Chernozem induced by glucose and N in relation to microbial growth strategies. *Appl. Soil Ecol.* **2007**, *37*, 95–105. [\[CrossRef\]](#)
60. Tambone, F.; Adani, F.; Gigliotti, G.; Volpe, D.; Fabbri, C.; Provenzano, M.R. Organic matter characterization during the anaerobic digestion of different biomasses by means of CPMA¹³C NMR spectroscopy. *Biomass Bioenergy* **2013**, *48*, 111–120. [\[CrossRef\]](#)
61. Tambone, F.; Orzi, V.; Zilio, M.; Adani, F. Measuring the organic amendment properties of the liquid fraction of digestate. *Waste Manag.* **2019**, *88*, 21–27. [\[CrossRef\]](#)
62. Tambone, F.; Scaglia, B.; D’Imporzano, G.; Schievano, A.; Orzi, V.; Salati, S.; Adani, F. Assessing amendment and fertilizing properties of digestates from anaerobic digestion through a comparative study with digested sludge and compost. *Chemosphere* **2010**, *81*, 577–583. [\[CrossRef\]](#)
63. Conde, E.; Cardenas, M.; Ponce-Mendoza, A.; Luna-Guido, M.L.; Cruz-Mondragón, C.; Dendooven, L. The impacts of inorganic nitrogen application on mineralization of ¹⁴C-labelled maize and glucose, and on priming effect in saline alkaline soil. *Soil Biol. Biochem.* **2005**, *37*, 681–691. [\[CrossRef\]](#)
64. Michel, J.; Hartley, I.P.; Buckeridge, K.M.; van Meegen, C.; Broyd, R.C.; Reinelt, L.; Quispe, A.J.C.; Whitaker, J. Preferential substrate use decreases priming effects in contrasting treeline soils. *Biogeochemistry* **2022**, *162*, 141–161. [\[CrossRef\]](#)

65. Liu, X.-J.A.; Sun, J.; Mau, R.L.; Finley, B.K.; Compson, Z.G.; van Gestel, N.; Brown, J.R.; Schwartz, E.; Dijkstra, P.; Hungate, B.A. Labile carbon input determines the direction and magnitude of the priming effect. *Appl. Soil Ecol.* **2017**, *109*, 7–13. [\[CrossRef\]](#)
66. Zhou, J.; Wen, Y.; Shi, L.; Marshall, M.R.; Kuzyakov, Y.; Blagodatskaya, E.; Zang, H. Strong priming of soil organic matter induced by frequent input of labile carbon. *Soil Biol. Biochem.* **2020**, *152*, 108069. [\[CrossRef\]](#)
67. Zhang, X.; Han, X.; Yu, W.; Wang, P.; Cheng, W. Priming effects on labile and stable soil organic carbon decomposition: Pulse dynamics over two years. *PLoS ONE* **2017**, *12*, e0184978. [\[CrossRef\]](#)
68. Bernard, L.; Basile-Doelsch, I.; Derrien, D.; Fanin, N.; Fontaine, S.; Guenet, B.; Karimi, B.; Marsden, C.; Maron, P. Advancing the mechanistic understanding of the priming effect on soil organic matter mineralisation. *Funct. Ecol.* **2022**, *36*, 1355–1377. [\[CrossRef\]](#)
69. Stewart, C.E.; Paustian, K.; Conant, R.T.; Plante, A.F.; Six, J. Soil carbon saturation: Concept, evidence and evaluation. *Biogeochemistry* **2007**, *86*, 19–31. [\[CrossRef\]](#)
70. Zomer, R.J.; Bossio, D.A.; Sommer, R.; Verchot, L.V. Global Sequestration Potential of Increased Organic Carbon in Cropland Soils. *Sci. Rep.* **2017**, *7*, 1–8. [\[CrossRef\]](#)
71. Cox, P.M.; Betts, R.A.; Jones, C.D.; Spall, S.A.; Totterdell, I.J. Acceleration of global warming due to carbon-cycle feedbacks in a coupled climate model. *Nature* **2000**, *408*, 184–187. [\[CrossRef\]](#)
72. Smith, P. Soils and climate change. *Curr. Opin. Environ. Sustain.* **2012**, *4*, 539–544. [\[CrossRef\]](#)
73. Gottschalk, P.; Smith, J.; Wattenbach, M.; Bellarby, J.; Stehfest, E.; Arnell, N.; Osborn, T.J.; Jones, C.; Smith, P. How will organic carbon stocks in mineral soils evolve under future climate? Global projections using RothC for a range of climate change scenarios. *Biogeosciences* **2012**, *9*, 3151–3171. [\[CrossRef\]](#)
74. Paustian, K.; Larson, E.; Kent, J.; Marx, E.; Swan, A. Soil C Sequestration as a Biological Negative Emission Strategy. *Front. Clim.* **2019**, *1*, 8. [\[CrossRef\]](#)
75. IPCC. *Working Group III Contribution to the IPCC Sixth Assessment Report (AR6)—Technical Summary*; IPCC: Geneva, Switzerland, 2021.
76. Sandén, T.; Spiegel, H.; Stüger, H.; Schlatter, N.; Haslmayr, H.; Zavattaro, L.; Grignani, C.; Bechini, L.; D'Hose, T.; Molendijk, L.; et al. European long-term field experiments: Knowledge gained about alternative management practices. *Soil Use Manag.* **2018**, *34*, 167–176. [\[CrossRef\]](#)
77. Haddaway, N.R.; Brown, C.; Eales, J.; Eggers, S.; Josefsson, J.; Kronvang, B.; Randall, N.P.; Uusi-Kämpä, J. The multifunctional roles of vegetated strips around and within agricultural fields. *Environ. Evid.* **2018**, *7*, 14. [\[CrossRef\]](#)
78. Riggers, C.; Poelau, C.; Don, A.; Frühauf, C.; Dechow, R. How much carbon input is required to preserve or increase projected soil organic carbon stocks in German croplands under climate change? *Plant Soil* **2021**, *460*, 417–433. [\[CrossRef\]](#)
79. Reuland, G.; Sigurnjak, I.; Dekker, H.; Michels, E.; Meers, E. The Potential of Digestate and the Liquid Fraction of Digestate as Chemical Fertiliser Substitutes under the RENDURE Criteria. *Agronomy* **2021**, *11*, 1374. [\[CrossRef\]](#)
80. National Inventory Report. *Belgium's Greenhouse Gas Inventory*; United Nations Framework Convention on Climate Change: New York, NY, USA, 2021.
81. van Wesemael, B.; Paustian, K.; Meersmans, J.; Goidts, E.; Barancikova, G.; Easter, M. Agricultural management explains historic changes in regional soil carbon stocks. *Proc. Natl. Acad. Sci. USA* **2010**, *107*, 14926–14930. [\[CrossRef\]](#)
82. Coppens, J.; Meers, E.; Boon, N.; Buysse, J.; Vlaeminck, S.E. Follow the N and P road: High-resolution nutrient flow analysis of the Flanders region as precursor for sustainable resource management. *Resour. Conserv. Recycl.* **2016**, *115*, 9–21. [\[CrossRef\]](#)
83. Papangelou, A.; Mathijs, E. Assessing agro-food system circularity using nutrient flows and budgets. *J. Environ. Manag.* **2021**, *288*, 112383. [\[CrossRef\]](#)
84. Evrard, O. Muddy Floods in the Belgian Loess Belt: Problems and Solutions. Ph.D. Thesis, Université Catholique de Louvain, Ottignies-Louvain-la-Neuve, Belgium, 2008; p. 222.
85. Minasny, B.; Malone, B.P.; McBratney, A.B.; Angers, D.A.; Arrouays, D.; Chambers, A.; Chaplot, V.; Chen, Z.-S.; Cheng, K.; Das, B.S.; et al. Soil carbon 4 per mille. *Geoderma* **2017**, *292*, 59–86. [\[CrossRef\]](#)
86. European Commission. *Nitrates Directive Implementation Report*; European Commission: Brussels, Belgium, 2018.
87. Lal, R. Digging deeper: A holistic perspective of factors affecting soil organic carbon sequestration in agroecosystems. *Glob. Chang. Biol.* **2018**, *24*, 3285–3301. [\[CrossRef\]](#)
88. Pastorelli, R.; Valboa, G.; Lagomarsino, A.; Fabiani, A.; Simoncini, S.; Zaghi, M.; Vignozzi, N. Recycling Biogas Digestate from Energy Crops: Effects on Soil Properties and Crop Productivity. *Appl. Sci.* **2021**, *11*, 750. [\[CrossRef\]](#)

Disclaimer/Publisher's Note: The statements, opinions and data contained in all publications are solely those of the individual author(s) and contributor(s) and not of MDPI and/or the editor(s). MDPI and/or the editor(s) disclaim responsibility for any injury to people or property resulting from any ideas, methods, instructions or products referred to in the content.